Since January 2020 Elsevier has created a COVID-19 resource centre with free information in English and Mandarin on the novel coronavirus COVID-19. The COVID-19 resource centre is hosted on Elsevier Connect, the company's public news and information website.

Antiviral Research 142 (2017) 1–11

Contents lists available at ScienceDirect

Antiviral Research

journal homepage: www.elsevier.com/locate/antiviral

Cellular protein GLTSCR2: A valuable target for the development of broad-spectrum antivirals

Cui-Cui Li [a, 1], Hui-Jun Dong [a, 1], Peng Wang [a, 1], Wen Meng [a, 1], Xiao-Jing Chi [b], Shi-Chong Han [a], Shuo Ning [a], Chuang Wang [a], Xiao-Jia Wang [a, *]

[a] Key Laboratory of Zoonosis of Ministry of Agriculture, College of Veterinary Medicine, China Agricultural University, Beijing, China
[b] Institute of Pathogen Biology, Chinese Academy of Medical Sciences, Beijing, China

ARTICLE INFO

Article history:
Received 30 September 2016
Received in revised form
20 January 2017
Accepted 2 March 2017
Available online 7 March 2017

Keywords:
GLTSCR2
Viral replication
DNA virus
RNA virus
shRNA

ABSTRACT

Viral infection induces translocation of the nucleolar protein GLTSCR2 from the nucleus to the cytoplasm, resulting in attenuation of the type I interferon IFN-β. Addressing the role of GLTSCR2 in viral replication, we detect that knocking down GLTSCR2 by shRNAs results in significant suppression of viral replication in mammalian and chicken cells. Injection of chicken embryo with the GLTSCR2-specific shRNA-1370 simultaneously or 24 h prior to infection with Newcastle disease virus (NDV) substantially reduces viral replication in chicken embryo fibroblasts. Injection of shRNA-1370 into chicken embryo also reduces the replication of avian influenza virus (AIV). In contrast, GLTSCR2-derived protein G4-T, forming α-helical dimers, increases replication of seven various DNA and RNA viruses in cells. Our studies reveal that alteration of the function of cellular GLTSCR2 plays a role in supporting viral replication. GLTSCR2 should be seriously considered as a therapeutic target for developing broad spectrum antiviral agents to effectively control viral infection.

1. Introduction

Type I interferon (IFN) cytokines are the first-line of defense against viral infections. They act through the immune system by rapidly inducting cellular modulators, thus inhibiting viral replication and spreading (Burke et al., 2014). Viral infections yield highly conserved pathogen-associated molecular patterns (PAMPs), such as double-stranded RNA (dsRNA). Viral RNA contains short hairpin dsRNA with triphosphorylated 5′ end (5′pppRNA) that preferentially activates host's pattern recognition receptors (PRRs), including the retinoic acid inducible gene-I (RIG-I) receptor (Ng and Gommerman, 2013). Tripartite motif (TRIM) proteins, TRIM25 (Gack et al., 2007) and TRIM4 (Yan et al., 2014), play a critical role in RIG-I activation through K63-linked ubiquitination. The activated RIG-I further interacts with mitochondrial antiviral-signaling protein (MAVS) and stimulates transcription factor, IFN regulatory factor-3/7 (IRF-3/7) to induce IFN gene expression (Wilkins and Gale, 2010). IFNs, secreted from virus-infected cells, bind to the IFN receptor (IFNAR) on the cell surface to initiate the JAK-STAT pathway. This upregulates hundreds of IFN-stimulated gene products (ISGs) and suppresses viral infection (Carty et al., 2014; Schneider et al., 2014). RIG-I agonists have been shown to induce IFN's expression and multiple innate antiviral response to control a number of viral infections. These include, vesicular stomatitis virus (VSV) of the family *Rhabdoviridae* (Goulet et al., 2013), hepatitis C virus (HCV) of the family *Flaviviridae* (Goulet et al., 2013), influenza virus of the family *Orthomyxoviridae* (Chiang et al., 2015), and herpes simplex virus type 1 (HSV-1) of the family *Herpesviridae* (Liu et al., 2016).

Viral infections, including rhabdovirus (Masatani et al., 2010), paramyxovirus (Ling et al., 2009), orthomyxovirus (Tawaratsumida et al., 2014), coronavirus (Xing et al., 2013), and herpesvirus (Xing et al., 2012), may counteract RIG-I-dependent IFN antiviral response. It has also been reported that viruses utilize the host cell's deubiquitinases and ubiquitin ligases to antagonize RIG-I-mediated innate immune response and succeed in viral replication. Cellular

Abbreviation: GLTSCR2, Glioma tumor suppressor candidate region gene 2; IFN-β, interferon β; shRNA, short hairpin RNA; $TCID_{50}$, 50% tissue culture infectious dose; HAU, hemagglutination unit; NDV, Newcastle disease virus; EV-A71, enterovirus A71; AIV, avian influenza virus; CDV, canine distemper virus; PEDV, porcine epidemic diarrhea virus; IBV, infectious bronchitis virus; VSV, vesicular stomatitis virus; HSV-1, herpes simplex virus type 1; HCV, hepatitis C virus.

* Corresponding author.
E-mail address: wangxj@cau.edu.cn (X.-J. Wang).

[1] Equally contributed.

http://dx.doi.org/10.1016/j.antiviral.2017.03.004
0166-3542/

ubiquitin-specific proteases, USP21 (Fan et al., 2014), USP3 (Cui et al., 2014) and USP15 (Zhang et al., 2015), a subfamily of deubiqutinase (Reyes-Turcu et al., 2009), remove K63-linked polyubiquitin chains from RIG-I and block it to induce IFN-β. Moreover, a cellular protein antagonizes the activation of RIG-I and participates in the innate immune response during viral infection. Such as Syndecan-4 (SDC4) and NOD-like receptor family CARD domain containing 5 (NLRC5) protein can interact with RIG-I to negatively regulate type I IFN antiviral response (Cui et al., 2010; Lin et al., 2016). The level of antiviral cytokines is significantly higher in USP21/SDC4- deficient mice. It should be noted that USP21/SDC4-deficient mice are more resistant to viral infection as compared with the control mice (Fan et al., 2014; Lin et al., 2016). It can thus be inferred that the depression of endogenous negative regulators of type I IFN exhibits a potential antiviral effect.

Glioma tumor suppressor candidate region gene 2 protein (GLTSCR2) is a nucleolar protein that contains multiple nucleolar localization sequences (Kalt et al., 2012). GLTSCR2 physically interacts with phosphatase and tensin homolog deleted on chromosome 10 (PTEN), and modulates programmed cell death (Okahara et al., 2004; Yim et al., 2007). Our previous study showed that viral infection induces translocation of GLTSCR2 from the nucleus to the cytoplasm. Cytoplasmic GLTSCR2 blocks IFN-β induction and deactivates RIG-I by negatively regulating it via K63-linked ubiquitination (Wang et al., 2016a). In present study, we find that purified G4-T, which mimics GLTSCR2 protein, promotes efficient proliferation of DNA and RNA viruses of distinct genera. We also develop a short hairpin RNA (shRNA) plasmid that targets a specific GLTSCR2 gene. Treatment of GLTSCR2-specific shRNA is found to significantly inhibit *in vitro* and *in vivo* infections. This paper provides solid evidence that GLTSCR2 is a valuable target for developing cell-based antivirals.

2. Materials and methods

2.1. Cells

HEp-2, HeLa, Vero, HEK293T, MDCK, and chicken embryo fibroblast DF-1 cells are cultured in Dulbecco's modified Eagle's medium (DMEM) supplemented with 2 mM L-glutamine, nonessential amino acids, sodium pyruvate, 5% or 10% heat-inactivated fetal bovine serum (FBS), 100 U/ml penicillin and 100 μg/ml streptomycin (all reagents are purchased from Gibco Invitrogen). Human hepatocellular liver carcinoma cell lines Huh7.5.1 are provided by Dr. Francis Chisari at Scripps Research Institute, Florida, USA. All cells are cultured at 37 °C in a humidified incubator with 5% CO_2.

2.2. Viruses

Enterovirus A71 (EV-A71) strain BC08 (Wang et al., 2012), avian influenza virus (AIV) strain H9-WD (Wang et al., 2016b), canine distemper virus (CDV) strain MD77 (Lan et al., 2005), Newcastle disease virus (NDV) strain Lasota and infectious bronchitis virus (IBV) strain M41 (Li et al., 2013), porcine epidemic diarrhea virus (PEDV) strain CV777 (Sun et al., 2015), VSV strain Indiana (Wang et al., 2016a), HSV-1 strain F (Wang et al., 2011) and HCV strain JFH-1 (Xu et al., 2014) are reproduced in RD, MDCK, Vero, HeLa, Vero, HeLa, HEK293T, HeLa and Huh7.5.1 cells respectively, according to the reports indicated above. GFP-NDV strain NA-1 is generated by inserting an additional transcription cassette coding for the enhanced GFP between the P and M genes of the NDV genome (Wang et al., 2015). The HCV genotype 1b replicon-containing cell line (2−3+) is provided by Dr. Stanley Lemon at University of Texas Medical Branch, USA (Yi and Lemon, 2004).

2.3. Antibodies

Rabbit polyclonal antibody to GLTSCR2 (used at 1:1000) is acquired from abcam. The anti NDV-P (1:1000), CDV-N (1:1000), VSV-G (1:200) mouse monoclonal antibodies are obtained from Santa Cruz. The antibodies to actin (1:1000) and His (1:1000) are obtained from Beyotime Biotechnology. The antibody to HCV-core (1:400) is preserved in our laboratory. Antibodies are diluted in PBS containing 5% skim milk (pH 7.3).

2.4. Protein production and purification

G4-T, in which HIV-derived cell-penetrating Tat peptide (Reissmann, 2014; Rizzuti et al., 2015) is conjugated at the C-terminal of G4, is constructed and cloned into the expression vector pET-28a *Nde*I-*Eco*RI restriction sites. *Escherichia coli* strain BL21(DE3) transformed with the recombinant His-tagged G4-T plasmid is grown at 37 °C in LB to an optical density of 0.8 (OD at 590 nm) before being induced with 1 mM IPTG for 4 h. Bacterial cells are harvested in PBS (pH 7.3) by centrifugation at 6000*g* for 20 min at 4 °C. The pellet is resuspended in 10 vol of pellet of lysis buffer (20 mM Tris-HCl, 100 mM NaCl, pH 8.0) in the presence of the protease inhibitor cocktail (Roche). After sonication, the cell suspension is fractionated by centrifugation at 6000g for 20 min at 4 °C. Supernatants (soluble fractions) are passed over to nickel-nitrilotriacetic acid (Ni-NTA) columns. Following the binding to column, the column is washed with lysis buffer containing increasing concentrations of imidazole (10, 20, 50, and 200 mM). His-fused protein G4-T is eluted and concentrated by ultrafiltration of 5 K membranes (Millipore), and stored at −80 °C.

2.5. Gel-filtration analysis

The purified G4-T protein eluted from His-Ni column is loaded onto the Superdex G200 column in a solution buffer of 20 mM Tris-HCl, pH 8.0. The analytical column is calibrated with a series of individual runs of standard molecular mass proteins as markers, including bovine serum albumin (68 kDa), egg white albumin (43 kDa), and ribose nucleotidase (13.7 kDa). The peak protein is collected and analyzed on 10% SDS-PAGE.

2.6. Chemical cross-linking

Purified protein G4-T is incubated at 4 °C in the presence of 0.05% Glutaraldehyde (GA, MP Biomedicals) for 15 min. The reaction is terminated by the addition of 200 mM Tris-HCl buffer, pH 8.0. Cross-linking products are analyzed by 10% SDS-PAGE and Western blotting.

2.7. Circular dichroism (CD) spectra analysis

The highly purified G4-T by the gel-filtration is incubated at the final concentration of 30 μM in PBS, with 0%, 25%, or 50% 2,2,2-trifluoroethanol (TFE). The wavelength-dependence of molar ellipticity [θ] is monitored at 25 °C as the average of eight scans in a spectropolarimeter (Model J-710, JASCO), equipped with a thermoelectric temperature controller. The thermal denaturation temperature (Tm) is measured at 222 nm by recording the CD signal in the temperature range of 20−75 °C with a scan rate of 1 °C/min.

2.8. Quantitative real-time PCR (RT-PCR)

Replicate cultures are harvested and total RNA is extracted with Trizol (Invitrogen). A two-step RT-PCR (SYBR Green I technology,

Applied Roche) is performed using SYBR green supermix (Toyobo) according to the manufacturer's protocol to measure transcription levels for several genes of interest. The primers used are as follows. IFN-β: 5′- CCT ACA AAG AAG CAG CAA-3′ (forward), 5′- TCC TCA GGG ATG TCA AAG -3′ (reverse). PKR: 5′- TAC GCC TGA CCA CAA CTA -3′ (forward), 5′- GGT ATT CCT TCC CGT CTA -3′ (reverse). ISG56: 5′- CAC CCA CTT CTG TCT TACT -3′ (forward), 5′- ACA TTC TTG CCA GGT CTA -3′ (reverse). NDV-N: 5′- TGA TGA CCC AGA AGA TAG ATG GAG -3′ (forward), 5′- CTG TGA GTG GGA GCA TAA AAG AGA -3′ (reverse). ICP8: 5′- GAC GGG CAA TCA GCG GTT CGC -3′ (forward), 5′- TCG TCC AGG TCG TCG TCA TCC -3′ (reverse). HCV-NS5A: 5′- TAG GTG CTG GGT CCA AATC -3′ (forward), 5′- TAT GCT GGC GAG GCT TAT -3′ (reverse). IBV-N: 5′- GGT TGC TGCT AAG GGT GC-3′ (forward), 5′- GCC TTT GTA ATG CGG GAG-3′ (reverse). GAPDH: 5′- CTG GTG ACC CGT GCT GCT T-3′ (forward), 5′- TTG CCG CCT TCT GCC TTA-3′ (reverse). Relative fold changes are automatically calculated by the Step One Plus real-time PCR system software (Applied Biosystems), following the $\Delta\Delta C_T$ method. GAPDH is also determined and used as internal control.

2.9. LDH assay for toxicity analysis

Protein cytotoxicity is assessed using a lactate dehydrogenase (LDH) assay according to the manufacturer's instructions by means of a Cytotoxicity Detection Kit^{PLUS} (Roche).

2.10. ELISA for IFN-β

HEK293T cells are infected with VSV at a MOI of 0.1 for indicated times, in the presence or absence of G4-T. The supernatants are harvested for ELISA (PBL Biomedical Laboratories) with a commercial sandwich kit (TFB), according to the manufacturer's instructions.

2.11. Preparation of cell lysates and immunoblots

The cells are harvested and dissolved in 200 μl lysis buffer (pH 7.5 20 mM Tris-HCl, 150 mM NaCl, 1% Triton X-100, 1 mM EDTA, 2.5 mM Sodium pyrophosphate, 1 mM β-Glycerrophosphate, 1 mM Sodium orthovanadate, 1 μg/ml Leupeptin) in the presence of the protease inhibitor cocktail for 30 min at 4 °C and finally disrupted by sonication. After then, the cell suspension is fractionated by centrifugation at 6000g for 20 min at 4 °C. Solubilized proteins are harvested, electrophoresed in denaturing polyacrylamide gels, transferred to a polyvinylidene fluoride membrane and reacted with the antibodies indicated. Protein bands are detected with secondary antibody conjugated to horseradish peroxidase (HRP), and actin is used as a loading control.

2.12. Determination of $TCID_{50}$

Cells are mock-infected or exposed to viruses in mixture supplemented with DMEM. After 90 min the inoculum is replaced with DMEM containing 2% FBS and incubated for 48 h or 72 h (only for HSV-1). Virus titration is performed in cells cultured in 96-well plate at 10^4 cells/well 24 h prior to the assay to achieve 80% confluency. Ten-fold serial dilutions are prepared for each sample and 100 μl/well of each dilution are added to the cells in quadruplicates. Wells with cytopathic effect are scored as positive for virus growth and $\log_{10}$ $TCID_{50}$/ml is determined by the method of Reed and Muench.

2.13. Reed and Muench method

Log_{10} 50% end point dilution = $\log_{10}$ of dilution showing a mortality next above 50% - (difference of logarithms × logarithm of dilution factor). Generally, the following formula is used to calculate “difference of logarithms” (difference of logarithms is also

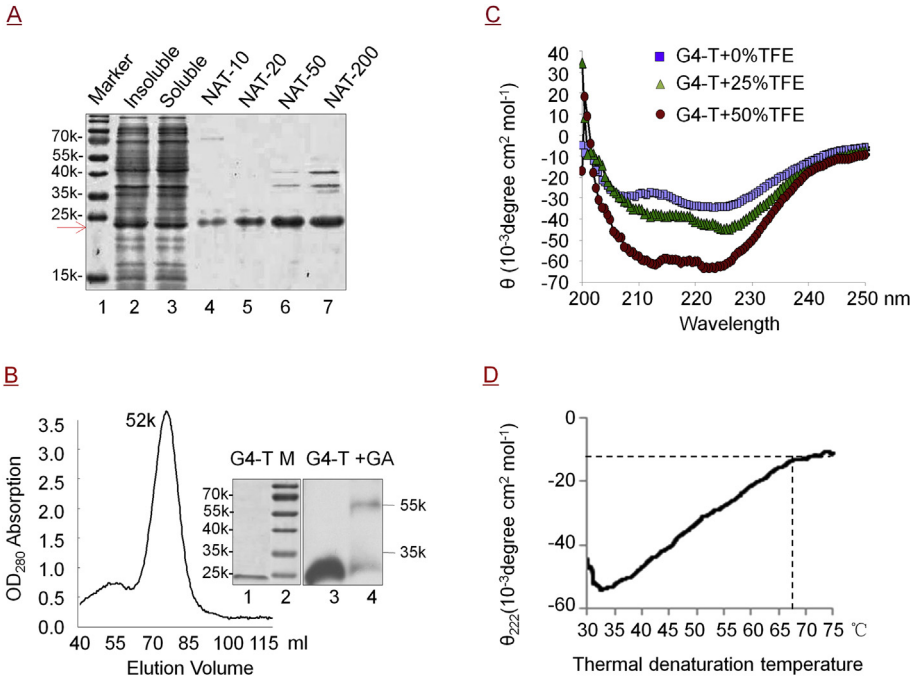

Fig. 1. Structural analysis of recombinant protein G4-T. ***(A)*** Production and purification of His-fusion G4-T. Lane 1, protein molecular-weight markers in kDa as indicated; lane 2–3, insoluble and soluble fractions of G4-T protein from *E. coli* lysate after sonication and centrifugation; lanes 4–7, G4-T was purified by His-Ni column with imidazole at concentrations of 10, 20, 50, and 200 mM. The fusion proteins were analyzed on 10% SDS-PAGE. ***(B)*** His-fusion G4-T was passed over the Superdex G200 column. The inset picture is 10% SDS-PAGE analysis of the peak protein (lane 1) and marker (lane 2), peak protein treated with 0% (lane 3) or 0.05% GA (lane 4) was analyzed by immunoblotting with antibody to His. ***(C)*** CD spectra of the purified G4-T in PBS solution with 0%, 25%, and 50% TFE. A typical α-helix secondary structure is showed with double minima at 208 and 222 nm. ***(D)*** Thermal denaturation of G4-T at wavelength of 222 nm.

known as “proportionate distance” or “interpolated value”): Difference of logarithms = [(mortality at dilution next above 50%)-50%]/[(mortality next above 50%)-(mortality next below 50%)].

2.14. HCV infectivity

HCV infectivity titers are determined by focus-forming units (FFU) assay. In brief, Huh7.5.1 cells seeded in a 96-well plate are infected with indicated MOI of HCV for different times. The number of FFU is counted automatically by an ImmunoSpot Series 5 UV Analyzer with customized software (CTL Europe GmbH). The viral infectivity titers in FFU/ml are averages from three independent assays.

2.15. siRNA interference

Cells in T-25 flask grown to 30–40% confluency are transfected with 200 pmol of siRNA (Santa Cruz) by using Lipofectamine™ 2000 (Invitrogen) according to manufacturer's protocols.

2.16. Design of shRNA

Invitrogen BLOCK-iT™ RNAi (https://rnaidesigner.thermofisher.com) is used to design siRNAs targeting Gallus GLTSCR2. Based on the siRNA screening results, shRNA-158, siRNA-243, and siRNA-1370 are predicted to have the best suppression effect and are selected to design shRNA. The shRNA sequences targeting Gallus GLTSCR2 are as follows (5′-3′; only the sense strand is shown). shRNA-158: GCG ATT TCC TCG AGG ATG TGA; shRNA-243: GGA TAC GGG CAA TGC TGA GAA; shRNA-1370: GCC TGA AGT ACG TGG AGA AGA. The shRNA expression vector pGPU6/GFP/Neo is selected to be the parental plasmid. All these DNA oligonucleotides are chemically synthesized by Invitrogen.

2.17. Transfection of shRNA plasmids

Cells grown to 60–80% confluency are transfected with plasmid-based shRNA by using Lipofectamine™ 2000 according to manufacturer's protocols.

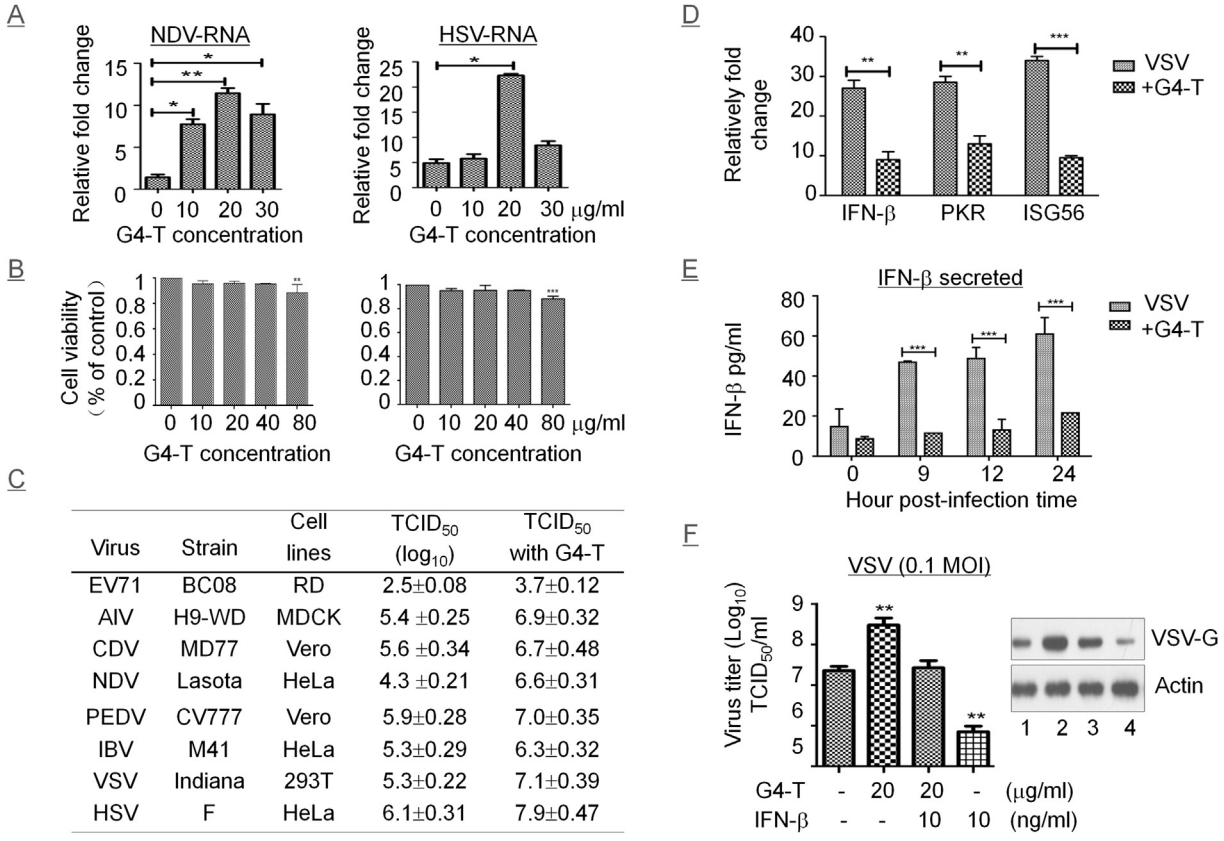

Virus	Strain	Cell lines	$TCID_{50}$ (log_{10})	$TCID_{50}$ with G4-T
EV71	BC08	RD	2.5±0.08	3.7±0.12
AIV	H9-WD	MDCK	5.4 ±0.25	6.9±0.32
CDV	MD77	Vero	5.6 ±0.34	6.7±0.48
NDV	Lasota	HeLa	4.3 ±0.21	6.6±0.31
PEDV	CV777	Vero	5.9±0.28	7.0±0.35
IBV	M41	HeLa	5.3±0.29	6.3±0.32
VSV	Indiana	293T	5.3±0.22	7.1±0.39
HSV	F	HeLa	6.1±0.31	7.9±0.47

Fig. 2. G4-T promoted the proliferation of viruses and suppressed the production and activity of IFN-β. ***(A)*** HEp-2 cells in T-25 flask were infected with NDV or HSV-1 of 10 PFU in the presence of G4-T at different concentrations of 0, 10, 20, and 30 μg/ml, NDV-N and HSV-ICP8 mRNA were quantified by RT-PCR at 48 h post-infection (h.p.i.). The values were normalized to the internal control (glyceraldehyde-3-phosphate dehydrogenase [GAPDH]) and expressed as relative fold changes over the control. These experiments were performed two times with three replicates in each experiment. Values represent means and standard deviations (SD). Statistical analysis was evaluated by one-way analysis of variance with Dunnett's multiple-comparison test. $^{*}p < 0.05$, $^{**}p < 0.01$ compared with control group. ***(B)*** Effects of G4-T on cell viability of cultured HEp-2 and Vero cells. Cells were treated with various concentrations of G4-T for 24 h, and cell viability was determined by LDH assay. These experiments were performed two times with three replicates in each experiment. Values represent means and SD. Statistical analysis was evaluated by one-way analysis of variance with Dunnett's multiple-comparison test. $^{**}p < 0.01$, $^{***}p < 0.001$ compared with control group. ***(C)*** Cells were infected with viruses at 10 $TCID_{50}$ or 1 $TCID_{50}$ (only for EV-A71) in the presence of PBS or G4-T (20 μg/ml) for 48 h or 72 h (only for HSV-1), virus titer was presented as log_{10} $TCID_{50}$/ml. These experiments were performed two times with three replicates in each experiment. Values represent means and SD. ***(D)*** HEK293T cells in T-25 flask were infected with VSV at a MOI of 0.1 for 12 h, in the presence of PBS or G4-T (20 μg/ml). Total RNA was isolated and used for quantification of IFN-β, PKR, and ISG56 mRNA levels by RT-PCR. These experiments were performed two times with three replicates in each experiment. Statistical analysis was evaluated by student's *t*-test. $^{**}p < 0.01$, $^{***}p < 0.001$ compared with PBS-treated group. ***(E)*** HEK293T cells in 24-well plate were infected with VSV at a MOI of 0.1 for indicated times, in the presence of PBS or G4-T (20 μg/ml). The supernatants from cells were harvested and analyzed for IFN-β production by ELISA. These experiments were performed two times with three replicates in each experiment. Statistical analysis was evaluated by student's *t*-test. $^{***}p < 0.001$ compared with PBS-treated group. ***(F)*** HEK293T cells were infected with VSV at a MOI of 0.1 in the presence of G4-T (20 μg/ml) (lanes 2–3) and commercially available IFN-β (10 ng/ml) (lanes 3–4), the virus yields were determined 48 h later, as log_{10} $TCID_{50}$/ml. These experiments were performed two times with three replicates in each experiment. Values represent means and SD. Statistical analysis was evaluated by one-way analysis of variance with Dunnett's multiple-comparison test. $^{**}p < 0.01$ compared with untreated group. Under the same experimental condition, electrophoretically separated proteins were analyzed by immunoblotting with specific antibody to viral protein VSV-G, with actin as a control (right).

2.18. SPF chicken embryo assay

For each inoculation, a mixture of shRNA plasmid (10 μg), Lipofectamine (10 μl), NDV (50 PFU, 50 μl) or AIV (500 PFU, 100 μl) is injected into the allantoic cavity of 9-day chicken eggs. Eggs are incubated for different times, and allantoic fluid is harvested to measure virus titer. All the embryos infected with NDV (50 PFU) or AIV (500 PFU) alive under the experimental condition.

2.19. Hemagglutination (HA) assay

Each allantoic fluid is collected and two-fold serially diluted in sterile saline; each dilution of 50 μl is reacted against an equal volume of 1% of washed red blood cells (RBC) of chicken. The maximum dilution of allantoic fluid that still results in complete agglutination of RBC suspension is recorded as HA unit (HAU). An experiment is performed three times, and the viral infectivity titers in HAU value are averages from two independent assays.

3. Results

3.1. Recombinant protein G4-T folds in an α-helical dimer structure

Previously, we showed that the C-terminal region G4 (amino acids 241–478) of GLTSCR2 participates in optimal VSV replication (Wang et al., 2016a). In the current study, His-fusion protein G4-T is produced, in which cell-penetrating peptide Tat (GGSRYGRKKRRQRRR) is conjugated at the C-terminal of G4. Recombinant protein G4-T is purified by Ni-column and eluted with a Tris-HCl buffer containing imidazole at concentrations of 10, 20, 50, or 200 mM. Results show that G4-T is highly soluble in 20 mM imidazole with over 85% purity at a concentration of about 1 mg/ml (Fig. 1A, lane 5). G4-T is then passed over a Superdex G200 column. This results in the self-association of G4-T into a dimer structure with a molecular mass of 52 kDa in a Tris-HCl buffer (Fig. 1B). Chemical cross-linking analysis confirms the formation of dimers of G4-T in the presence of 0.05% Glutaraldehyde (GA) (lane 4).

Circular dichroism (CD) spectrometry is performed to study the secondary structural changes in PBS with and without 2,2,2-trifluoroethanol (TFE). TFE is widely used in conformational studies because it promotes intramolecular hydrogen bonds in spite of intermolecular interactions with water molecules, and thus, lowers the polarity of the solution (Chi et al., 2013). Results show that G4-T protein exhibits a tendency to form a α-helical secondary structure in a PBS buffer solution. The tendency to form α-helical secondary structure for G4-T protein in the presence of 25% and 50% TFE is more obvious than that in the absence of TFE (Fig. 1C). This result indicates that there is no effect of polarity on

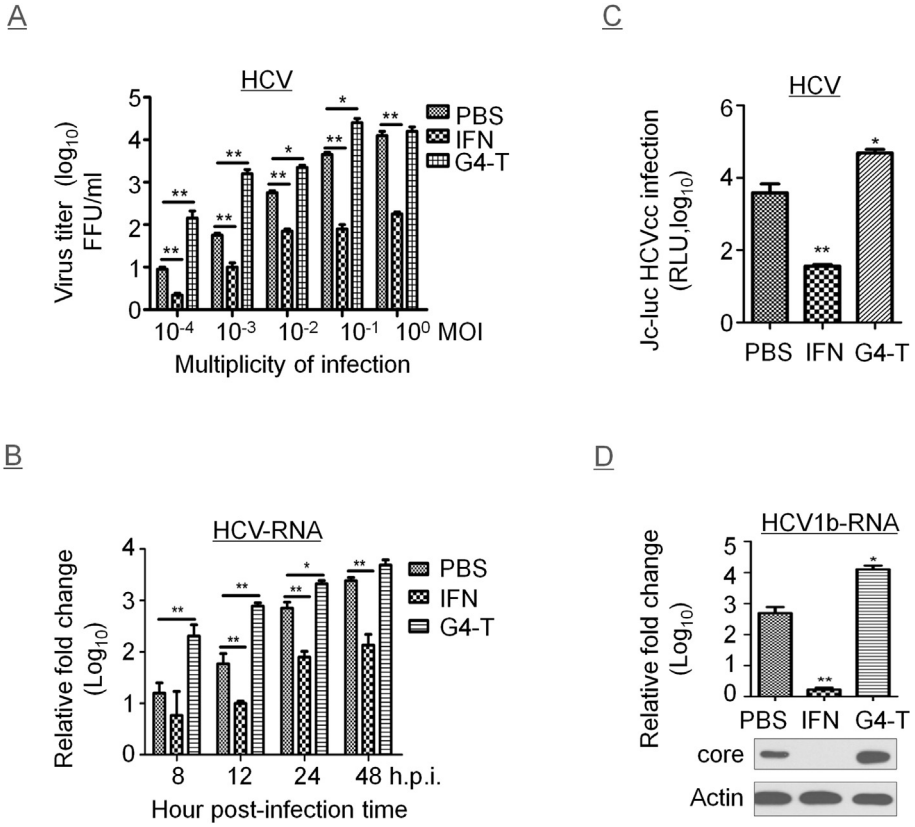

Fig. 3. G4-T promoted fast and efficient replication of HCV. ***(A)*** Huh7.5.1 cells were exposed to HCV at a MOI of 0.0001, 0.001, 0.01, 0.1, 1.0, in the presence of G4-T (20 μg/ml), IFN-β (10 ng/ml), or PBS for 48 h. Virus titer was presented as $\log_{10}$ FFU/ml. Statistical analysis was evaluated by two-way analysis of variance with Dunnett's multiple-comparison test. ***(B)*** Huh7.5.1 cells were exposed to HCV at a MOI of 0.1 for indicated times, in the presence of G4-T, IFN-β, or PBS. Total RNA was isolated; HCV-NS5A mRNA was quantified by RT-PCR, and assessed as described in Fig. 2A. Statistical analysis was evaluated by two-way analysis of variance with Dunnett's multiple-comparison test. ***(C)*** Huh7.5.1 cells were transfected with the linear Jc1-Luc HCV plasmid for 48 h, in the presence of G4-T, IFN-β, or PBS. The cells were lysed and assayed with luciferase assay system in a Modulus Microplate Luminometer. We typically obtain counts ranging from 10,000–900,000, whereas the background signal from bald virus infected sample is usually below 100. Statistical analysis was evaluated by one-way analysis of variance with Dunnett's multiple-comparison test. $^{*}p < 0.05$, $^{**}p < 0.01$ compared with PBS-treated group. ***(D)*** The HCV genotype 1b replicon-containing cell line (2−3+) was seeded as triplicates in 48-well plate the day before treated for 48 h, in the presence of G4-T, IFN-β, or PBS. Total RNA was isolated; HCV-NS5A mRNA was quantified by RT-PCR, and assessed as described in Fig. 3B. Statistical analysis was evaluated by one-way analysis of variance with Dunnett's multiple-comparison test. The cells were also harvested and immunoblotted with antibody to viral protein HCV-core, with actin as a control. All the experiments were performed at least two times with three replicates in each experiment. Values represent means and SD. $^{*}p < 0.05$, $^{**}p < 0.01$ compared with PBS-treated group.

protein conformation when G4-T is transferred from water to membrane interfaces. The α-helix structure, however, disappears when the temperature exceeds 65 °C (Fig. 1D).

3.2. G4-T promotes efficient proliferation of viruses belonging to 6 families

To explore if G4-T protein promotes efficient proliferation of viruses, cells infected with Newcastle disease virus (NDV) and HSV-1 are treated with G4-T at concentrations of 10, 20, and 30 μg/ml. As shown in Fig. 2A, G4-T protein increases the expression level of NDV-N and HSV-ICP8 mRNA; the level being dependent on the dose. 4–6 fold increase in mRNA level is observed when treated with G4-T at the concentration of 20 μg/ml. To investigate whether G4-T protein has a toxic effect on cells, HEp-2 and Vero cells are cultured in a medium containing different concentrations (0, 10, 20, and 40 μg/ml) of G4-T protein for 24 h. Cell viability is then assessed using LDH assay. No significant difference is observed between untreated and G4-T treated cells (Fig. 2B). The cell lines are then treated with G4-T at 20 μg/ml and $TCID_{50}$ is measured following virus infections. As shown in Fig. 2C, G4-T increases virus yield in $TCID_{50}$ by 16, 32, 13, 208, 13, 10, 62, and 58 folds, as compared with cells infected in a controlled manner with EV-A71, AIV, CDV, clinically new isolated NDV, PEDV, IBV, VSV, and HSV-1, respectively.

3.3. G4-T suppresses type I IFN antiviral response

To examine if G4-T promotes proliferation of viruses by abrogating the expression of type I IFN, we measure the mRNA levels of IFN-β, PKR, and ISG56. As shown in Fig. 2D, there is a 2–3 fold reduction in mRNA level when treated with G4-T protein at 20 μg/ml. In addition, HEK293T cells treated with G4-T protein and infected with VSV for 9, 12, and 24 h, show significantly reduced levels of IFN-β secretion (Fig. 2E). It is also observed that G4-T increases VSV yield in $TCID_{50}$ by 30 folds, and increases the expression level of VSV-G (Fig. 2F, lane 2). Commercially available IFN-β at a concentration of 10 ng/ml decreases the virus titer and expression of VSV-G enhanced by G4-T (lane 3). These results indicate that G4-T protein sensitizes host cells to the virus by suppressing their antiviral response.

3.4. G4-T promotes fast and efficient proliferation of HCV

To explore if G4-T protein promotes viral proliferation, three well-established HCV infectivity assays are performed. Our results

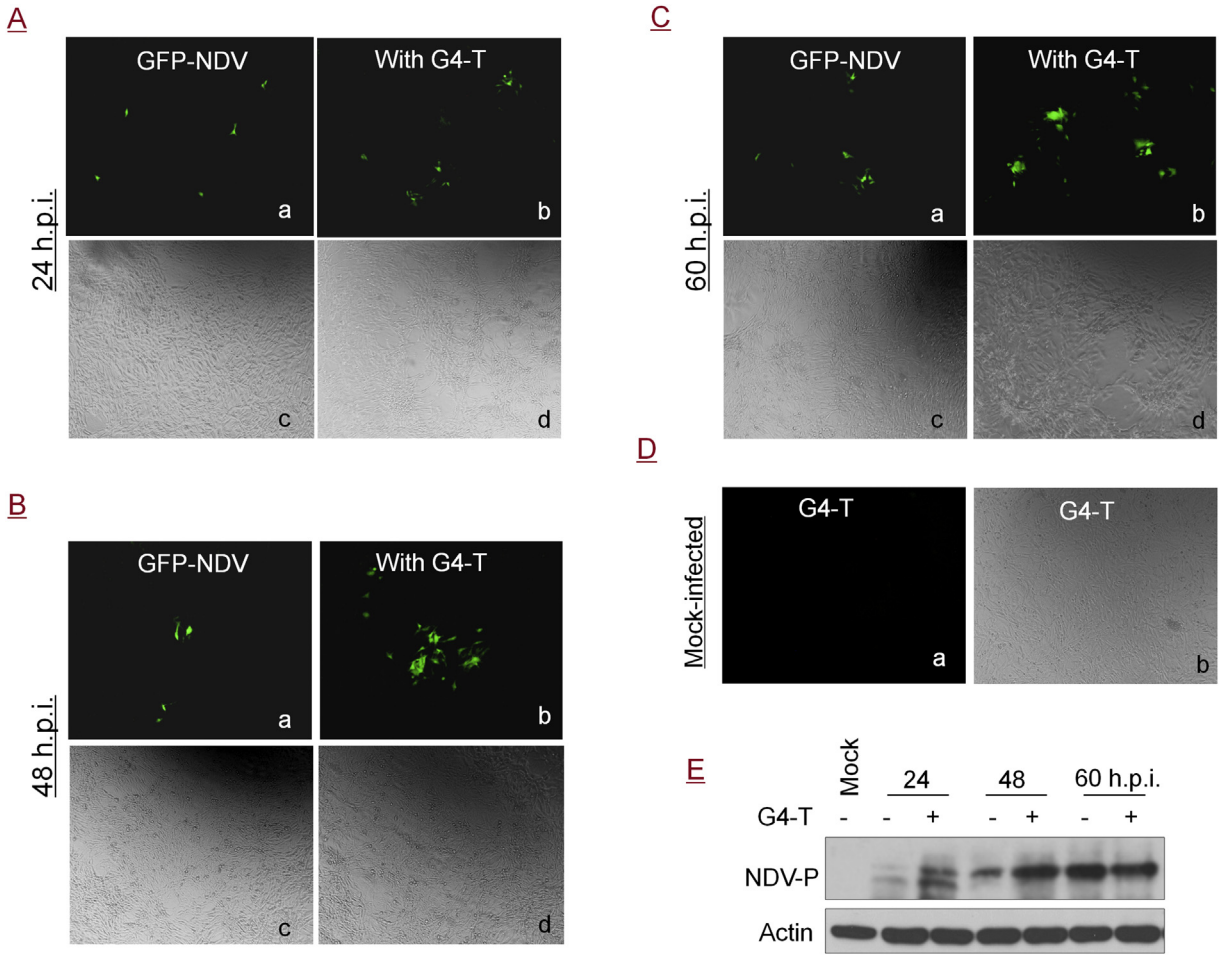

Fig. 4. G4-T affected syncytium number and viral replication of GFP-NDV. DF-1 cells in 48-well plate were exposed to GFP-NDV of 10 $TCID_{50}$ for 24 h ***(A)***, 48 h ***(B)***, and 60 h ***(C)***, in the presence of PBS or G4-T (20 μg/ml). The syncytiums were imaged using a DP73 camera by fluorescence microscopy on an Olympus IX73 microscope 25 (magnification of 100×) (panels a–b), and were assessed under light microscopy (panels c–d). One image is representative of three. ***(D)*** DF-1 cells were treated with G4-T (20 μg/ml) for 60 h, then were imaged by fluorescence microscopy (panel a) and light microscopy (panel b). ***(E)*** DF-1 cells in T-25 flask were infected with GFP-NDV of 100 $TCID_{50}$ in the presence of PBS or G4-T (20 μg/ml). At 24, 48, and 60 h.p.i., cells were harvested and electrophoretically separated proteins were analyzed by immunoblotting with antibody to viral protein NDV-P, with actin as a control.

show that G4-T at 20 μg/ml increases HCV yield in FFU by 10–50 folds over a broad MOI range from 0.0001 to 0.1. However, G4-T does not play a role at MOI of 1 (Fig. 3A). We also explored the effect of G4-T on the expression of viral mRNA throughout the entire infection course. As shown in Fig. 3B, G4-T significantly enhances the intracellular level of HCV-NS5A mRNA at 8, 12, and 24 h post-infection (h.p.i.). We also find that the expression levels of HCV-NS5A mRNA present in a similar manner in the presence and absence of G4-T at 12 h.p.i. and 24 h.p.i., respectively. A similar behavior is observed in the presence of G4-T at 24 h.p.i. and in the absence of G4-T at 48 h.p.i. (Fig. 3B). The results shown in Fig. 3A and B indicate that G4-T promotes efficient replication of HCV in a virus titer in a time-dependent manner. Furthermore, Huh7.5.1 cells are transfected with the linear Jc1-Luc HCV plasmid, followed by treatment with G4-T protein; cell lysates are subjected to luciferase assay. The result shows that G4-T improves *in vitro* transcription of Jc1-Luc HCV (Fig. 3C). Finally, the HCV genotype 1b replicon-containing cell line (2–3+) is seeded in the presence of G4-T. We observe that G4-T up-regulates the expression of HCV-core (Fig. 3D). Based on the above results, we can conclude that G4-T treatment is associated with a more efficient replication of HCV.

3.5. G4-T promotes viral proliferation of GFP-NDV

To quantify the effect of G4-T treatment on the efficiency with which virus infection induces syncytium formation, cells are infected with a recombinant NDV expressing the green fluorescent protein (GFP) and cultured for 24, 48, and 60 h. The syncytiums number is then analyzed by fluorescence microscopy. As shown in Fig. 4A–C, GFP-NDV produces a larger number of syncytiums in cells treated with G4-T at 20 μg/ml as compared to those not treated with G4-T. These results demonstrate that the G4-T protein plays a significant role in promoting the spreading of the virus. In addition, G4-T treatment for 60 h does not induce syncytium formation (Fig. 4D). Viral replication is further confirmed by examining the expression of NDV-P. As shown in Fig. 4E, G4-T significantly promotes viral replication at 24 and 48 h.p.i., but is ineffective at 60 h.p.i. These results indicate that G4-T protein enhances the spreading and replication of GFP-NDV in a time-dependent manner.

3.6. GLTSCR2 knockdown reduces viral infection in mammalian and chicken cells

Our previous study showed that GLTSCR2 knockdown results in a reduced production of viral particles of VSV, NDV, and IBV by 60, 120, and 20 folds, respectively (Wang et al., 2016a). In the present study, commercially available small interfering RNA (siRNA), which targets GLTSCR2 gene, efficiently suppresses mRNA levels of viral proteins of NDV-N (Fig. 5A), IBV-N (Fig. 5B), and HSV-ICP8 (Fig. 5C)

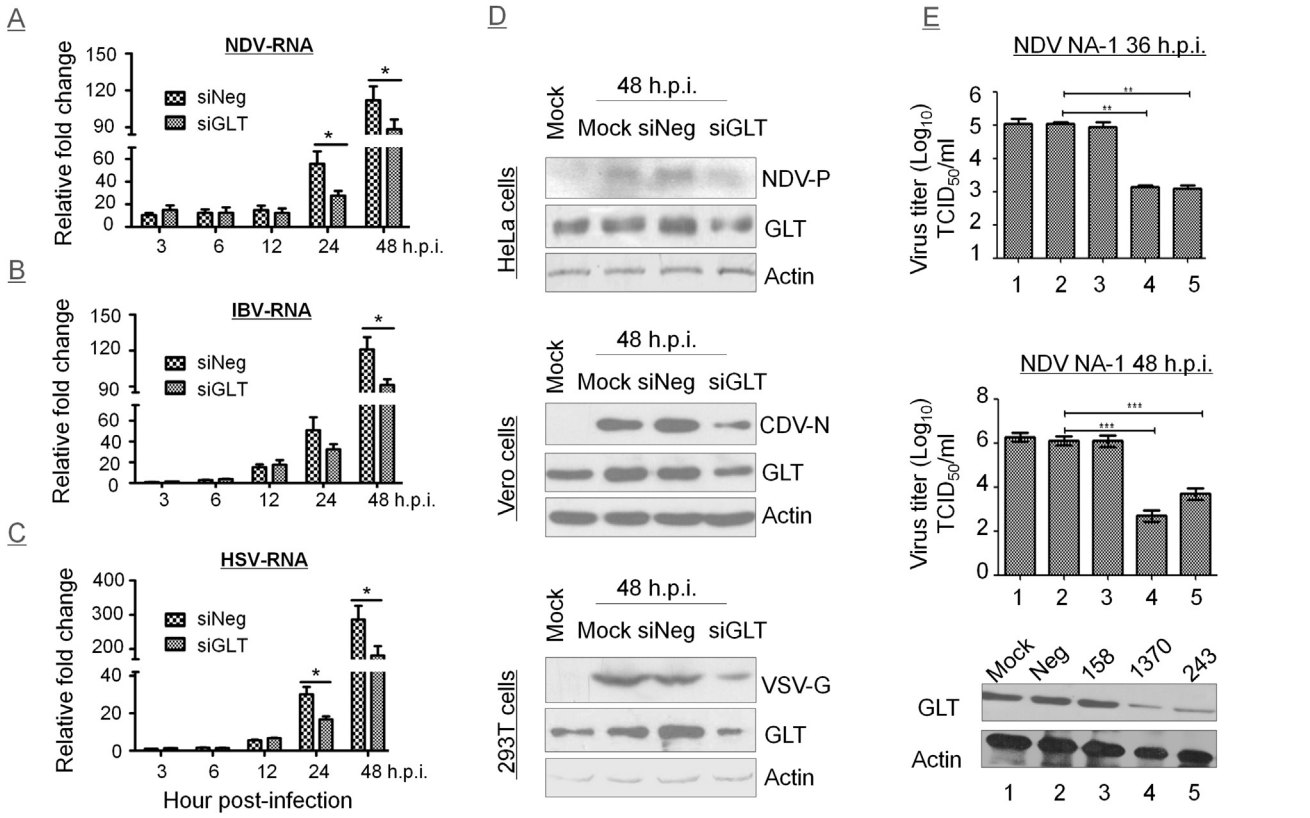

Fig. 5. Effect of GLTSCR2 knockdown on viral replications in cells. HEp-2 cells in T-25 flask were transfected with negative siRNA or siRNA targeting GLTSCR2 for 72 h, subsequently were infected with NDV (strain Lasota), IBV, and HSV-1 of 10 PFU for indicated times. Total RNA was isolated; NDV-N ***(A)***, IBV-N ***(B)***, and HSV- ICP8 ***(C)*** mRNA were quantified by RT-PCR, and assessed as described in Fig. 2A. These experiments were performed two times with three replicates in each experiment. Values represent means and SD. Statistical analysis was evaluated by student's *t*-test. $^{*}p < 0.05$ compared with negative siRNA-treated group. ***(D)*** HeLa, Vero, and HEK293T cells in T-25 flask were transfected with negative siRNA or siRNA (200 pmol each) targeting GLTSCR2 for 72 h, subsequently were infected with NDV (strain Lasota), CDV, and VSV of 10 PFU for 48 h. Electrophoretically separated proteins were immunoblotted with indicated antibodies, with actin as a control. ***(E)*** The shRNA-expressing plasmids (5 μg each) were transfected into DF-1 cells in 6-well plate for 96 h, and then infected with GFP-NDV (strain NA-1) of 50 $TCID_{50}$. At 36 and 48 h.p.i., DF-1 cells were harvested and virus titer was presented as $\log_{10}$ $TCID_{50}$/ml. These experiments were performed two times with three replicates in each experiment. Values represent means and SD. Statistical analysis was evaluated by one-way analysis of variance with Dunnett's multiple-comparison test. $^{**}p < 0.01$, $^{***}p < 0.001$ compared with negative shRNA-treated group. Efficiency of knockdown was analyzed by immunoblotting with specific antibody to GLTSCR2, with actin as a control (bottom).

in HEp-2 cells. GLTSCR2-specific siRNA is also able to suppress the expression of NDV-P, CDV-N, and VSV-G in HeLa, Vero, and HEK293T cells, respectively (Fig. 5D). This result indicates that GLTSCR2 knockdown inhibits the replication of multiple viruses.

Newcastle disease is one of the most important avian diseases in poultry. Virulent variant strains of NDV are sporadically isolated from vaccinated chickens, wild birds, and even swine (Yuan et al., 2012). In the present research effort, chicken embryo fibroblast DF-1 cells are transfected with recombinant plasmids carrying shRNA that are designed to target GLTSCR2, i.e., shRNA-158, shRNA-243, and shRNA-1370. As shown in Fig. 5E, shRNA-243 and shRNA-1370 reduces virus titer in $TCID_{50}$ by 100 folds at 36 h.p.i., and by 250 and 1000 folds at 48 h.p.i., respectively. shRNA-158 does not significantly affect the virus titer. It can be concluded that GLTSCR2 knockdown reduces viral infection in mammalian and chicken cells. These results also indicate that shRNA-1370 exhibits stronger inhibition characteristics as compared with shRNA-243 treatment.

3.7. GLTSCR2-specific shRNAs reduce GFP-NDV infection in chicken embryos

We further examined the ability of shRNA expression plasmid of shRNA-1370, which targeting Gallus GLTSCR2 (nucleic acid 1370–1390), to reduce GFP-NDV proliferation in chicken embryos. This is widely used *in vivo* model of viral infection, especially for NDV (Yue et al., 2009) and influenza virus (Ge et al., 2003). GFP-NDV and shRNA-1370 are injected with lipofectamine of a lipid-based carrier into the allantoic cavity of 9-day-old specific pathogen-free (SPF) chicken embryos. Allantoic fluids are harvested 36, 48, 60, 72, 84, and 96 h post infection to measure virus titers in DF-1 cells. We detect that treatment with 2.5 μg of shRNA-1370 does not affect the virus titer, while 5 μg of shRNA-1370 has a slight effect on it (not shown here). 10 μg of GLTSCR-specific shRNA provides the optimal inhibitory activity and is administered in subsequent experiments.

Our results demonstrate that treatment with shRNA-1370 at 24 h prior to (Fig. 6) or simultaneous (Fig. 7) infection with GFP-NDV results in the reduced production of viral particles. Injection of chicken embryo with the GLTSCR2-specific shRNA-1370 at 24 h prior to infection with NDV decreases the virus titer in $TCID_{50}$ by 4, 3, 7, 6, 13, and 61 folds (Fig. 6); while a simultaneous shRNA-1370 treatment with NDV infection reduces $TCID_{50}$ by 6, 4, 20, 29, 17, and 66 folds, at 36, 48, 60, 72, 84, and 96 h.p.i., respectively (Fig. 7). In summary, shRNA-1370 effectively reduces NDV replication in

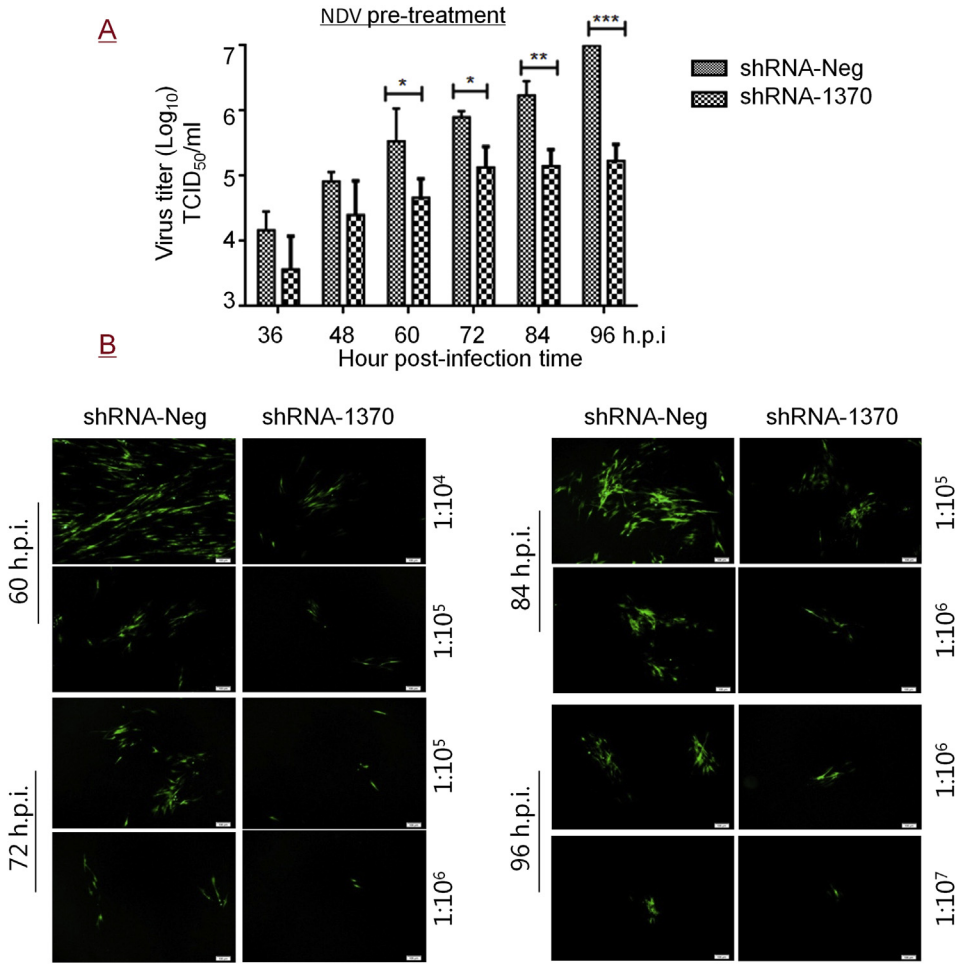

Fig. 6. Pre-treatment of GLTSCR2-specific shRNA-1370 reduced GFP-NDV infection in chicken embryos. ***(A)*** Each shRNA (shRNA-1370, shRNA-Neg) (10 μg each) was injected into the allantoic cavity of a 9-day-old SPF chicken egg used 24 h prior to GFP-NDV inoculation (50 PFU). The eggs were incubated at 37 °C for 36, 48, 60, 72, 84, and 96 h with observation every 6 h. The eggs were stored immediately at 4 °C every 12 h, and all eggs were harvested and analyzed at the same time. The virus titer of allantoic fluid was determined as $\log_{10}$ $TCID_{50}$/ml by fluorescence microscopy in DF-1 cells. These experiments were performed two times with three replicates in each experiment. Values represent means and SD. Statistical analysis was evaluated by two-way analysis of variance with Bonferroni's multiple comparisons test. $^{*}p < 0.05$, $^{**}p < 0.01$, $^{***}p < 0.001$ compared with negative shRNA-treated eggs. ***(B)*** Specific fluorescence in DF-1 cells infected with GFP-NDV was imaged by fluorescence microscopy (magnification of 100×), one image is representative of three. The description ($1{:}10^4$, $1{:}10^5$, $1{:}10^6$, and $1{:}10^7$) indicated the dilution of NDV-infected allantoic fluid used for inoculation of cells.

chicken embryos.

3.8. GLTSCR2-specific shRNA-1370 reduces AIV infection in chicken embryos

To study the effect of shRNA-1370 on AIV infection in SPF chicken embryos, virus titers from allantoic fluids of chicken embryos are measured by HA assay. As shown as in Fig. 8A, shRNA-1370 treatment at 24 h prior to infection with AIV reduces HAU value by 3 folds at 96 h.p.i. However, it does not significantly affect the virus titer at 36, 48, and 72 h.p.i. In contrast, simultaneous shRNA-1370 treatment with AIV infection reduces HAU value by 2, 4, and 3 folds at 48, 72, and 96 h.p.i. Our results demonstrate that shRNA-1370 effectively interferes with AIV proliferation in chicken embryos.

4. Discussion

Virus cultivation still remains a major challenge in the field of general virology because viral propagation is difficult and time consuming, especially for the novel clinically isolated and re-emerging viruses. Several studies, including the ones conducted by Andrejeva et al., 2002 and Hilton et al., 2006, have shown that viral proteins may counteract IFN antiviral response to facilitate their replication. The permanent cell lines stably expressing these viral proteins have been established for optimal in replication of viruses including paramyxovirus (Young et al., 2003) and herpesviruses (Everett et al., 2008; McSharry et al., 2015). It is thus inferred that if the accumulation of negative regulators of type I IFN is increased in cells, they are more susceptible to virus infection than the parent control cells. In the present study, we address the key challenges that remain towards developing more efficient virus cultivation, and establish a simple approach that substantially inoculate viruses by directly adding recombinant protein G4-T in a culture medium of mammalian cells. G4-T protein, a negative regulator of type I IFN, can promote efficient proliferation of at least 9 laboratory adapted and clinically isolated viruses, including the families, *Rhabdoviridae* (VSV), *Orthomyxoviridae* (AIV), *Paramyxoviridae* (NDV, CDV), *Coronaviridae* (PEDV, IBV), *Picornaviridae* (EV-A71), *Flaviviridae* (HCV), and *Herpesviridae* (HSV-1). This work provides a feasible countermeasure for optimizing viral replication for both enveloped and non-enveloped DNA and RNA viruses. G4-T

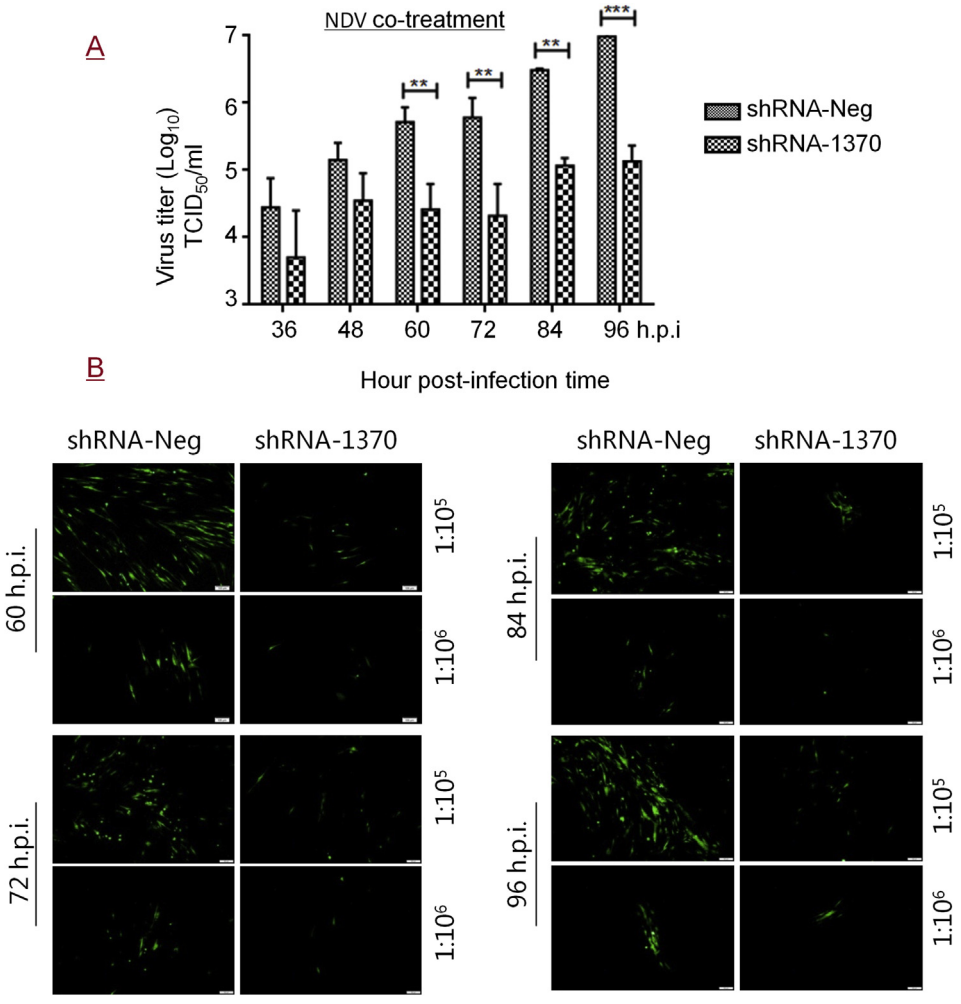

Fig. 7. Co-treatment of shRNA-1370 reduced GFP-NDV infection in chicken embryos. ***(A)*** Each shRNA (shRNA-1370, shRNA-Neg) (10 μg each) was injected into the allantoic cavity of a 9-day-old SPF chicken egg simultaneously with GFP-NDV inoculation (50 PFU). The egg were incubated for 36, 48, 60, 72, 84, and 96 h and analyzed at the same time. The virus titer in allantoic fluid was determined as $\log_{10}$ $TCID_{50}$/ml by fluorescence microscopy in DF-1 cells. These experiments were performed two times with three replicates in each experiment. Values represent means and SD. Statistical analysis was evaluated by two-way analysis of variance with Bonferroni's multiple comparisons test. $^{**}p < 0.01$, $^{***}p < 0.001$ compared with negative shRNA-treated eggs. ***(B)*** Specific fluorescence in DF-1 cells infected with GFP-NDV was imaged by fluorescence microscopy (magnification of 100×), one image is representative of three. The description ($1{:}10^5$ and $1{:}10^6$) indicated the dilution of NDV-infected allantoic fluid used for inoculation of cells.

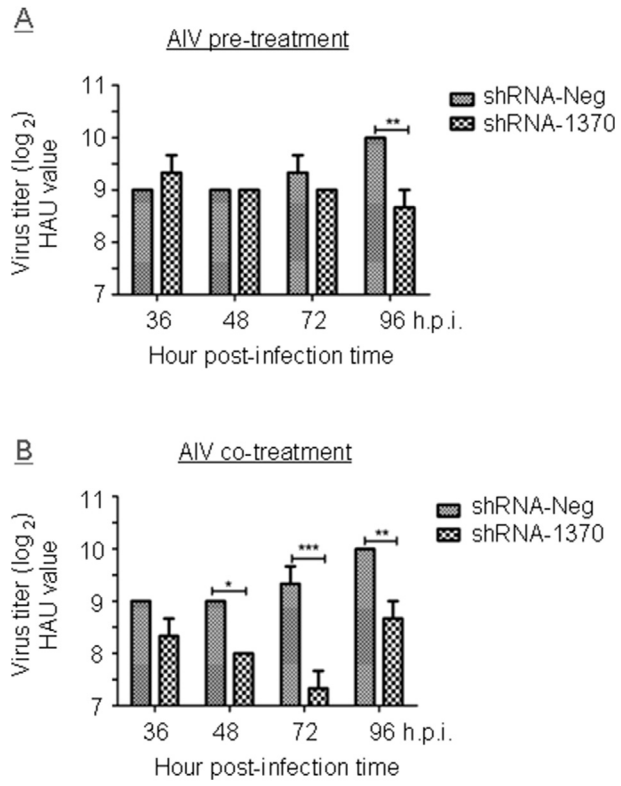

Fig. 8. GLTSCR2-specific shRNA-1370 reduced AIV infection in chicken embryos. The shRNA-1370 or shRNA-Neg (10 μg each) was injected into the allantoic cavity of a 9-day-old SPF chicken eggs used 24 h prior to ***(A)*** or simultaneously ***(B)*** infection with AIV (500 PFU). After shRNA injection and virus inoculation, the eggs were incubated for 36, 48, 72, and 96 h. Virus titers in allantoic fluids were determined as $\log_2$ HAU/50 μl. These experiments were performed two times with three replicates in each experiment. Values represent means and SD. Statistical analysis was evaluated by two-way analysis of variance with Bonferroni's multiple comparisons test. $^{*}p < 0.05$, $^{**}p < 0.01$, $^{***}p < 0.001$ compared with negative shRNA-treated eggs.

protein is expected to treat viruses in clinical samples that are fastidious and difficult to cultivate, and vaccine strains from wild-type isolates. Our study highlights the potential of the cellular protein GLTSCR2 to be a valuable target for the development of broad-spectrum class of antivirals.

Over the past 10 years numerous applications have successfully used the RNA interference (RNAi) technology. It is based on the fact that small interfering RNA (siRNA) molecules or short hairpin RNAs (shRNAs) target viral and cellular mRNA, which results in the degradation and suppression of specific gene expressions (Bosher and Labouesse, 2000; Das et al., 2006). The development of the plasmid-based technology to produce shRNA, driven by the U6 promoter, has made long term and inducible gene silencing possible (Sui et al., 2002). A number of studies have demonstrated that RNAi-mediated gene suppression of pathogenic viruses to be highly effective against many human and animal viruses both *in vitro* and *in vivo* (Burnett et al., 2011; DeVincenzo, 2012; Huang, 2008; Jain and Jain, 2015; Spurgers et al., 2008). The siRNA- and shRNA-mediated knockdown can inhibit viral replication of NDV and AIV in chicken cells and embryos. The plasmid-based shRNA that targets matrix protein M of NDV (Yin et al., 2010) and nucleocapsid protein NP of AIV (Abrahamyan et al., 2009) leads to a yield reduction of 80 and 400 folds in cells, respectively. Furthermore, shRNA targets NP of NDV that is delivered into the chicken embryos and reduces HA value by 10 folds in virus titer (Yue et al., 2009), while siRNA targets NP of AIV and reduces HAU value by 8 folds (Ge et al., 2003).

In this study, GLTSCR2-specific shRNA-1370 is evaluated for antiviral activity against NDV and AIV by means of virus titration in chicken cells and embryos. Our results show that plasmid-based shRNA-1370 induces up to 1000-fold decrease in the infective titer in cells infected with NDV (Fig. 5). In our chicken embryo experiments, NDV of 50 PFU in 50 μl has been selected to inject into the allantoic cavity of 9-day chicken eggs. Infected eggs are stored immediately at 4 °C for 12 h, and all eggs are harvested and analyzed simultaneously for consistency. Under this experimental condition, NDV titer reaches the peak at 96 h.p.i. As shown in Figs. 6–8, application of shRNA-1370 substantially reduces viral replication of NDV and AIV in chicken embryo fibroblasts. There are two time milestones that are noteworthy. At 96 h.p.i, the case with a shRNA-1370 treatment simultaneously or 24 h prior to infection with NDV substantially reduces the virus titer in $TCID_{50}$ by over 60 folds, and in HAU value by 3 folds for AIV. It is suggested that the shRNA-1370 treatment has substantial effect on viral replication. The impact is stronger with increasing treatment time. At 72 h.p.i, beyond our expectation, a simultaneous shRNA-1370 treatment with NDV infection reduces the virus titer in $TCID_{50}$ by 29 folds, and in HAU value by 4 folds for AIV. The antiviral effect at 72 h.p.i. is more prominent than that at 48, 60, and 84 h.p.i. This interesting issue remains to be addressed. There is limited literature describing shRNA plasmid-based platforms that target cellular proteins utilized by viruses for *in vivo* proliferation. Our study provides a model for the screening and identification of cell-based antivirals. This work also provides a new idea for the design of an intervention strategy against multiple viruses by targeting negative feedback regulators of type I IFN.

Colon and esophageal cancers in humans that harbor low levels of GLTSCR2 show a better 5-year survival rate than patients whose cancers have high GLTSCR2 levels (Sasaki et al., 2011). Therefore, small molecule inhibitors that are designed based on GLTSCR2-specific shRNA are expected to act as broad therapy against viral infection, without cytotoxicity and side-effects on host cells. We are currently investigating structure-based design of small molecule antagonist.

Author contributions

C.C.L., H.J.D., P.W., W.M. and X.J.W. analyzed data; all performed research; and X.J.W. designed research and wrote the paper.

Acknowledgments

This work is supported by the National Natural Science Foundation of China (31572515), and by the Beijing Natural Science Foundation of China, Grant No. 6142013.

References

Abrahamyan, A., Nagy, E., Golovan, S.P., 2009. Human H1 promoter expressed short hairpin RNAs (shRNAs) suppress avian influenza virus replication in chicken CH-SAH and canine MDCK cells. Antivir. Res. 84, 159–167.
Andrejeva, J., Young, D.F., Goodbourn, S., Randall, R.E., 2002. Degradation of STAT1 and STAT2 by the V proteins of simian virus 5 and human parainfluenza virus type 2, Respectively: consequences for virus replication in the presence of alpha/beta and gamma interferons. J. Virol. 76, 2159–2167.
Bosher, J.M., Labouesse, M., 2000. RNA interference: genetic wand and genetic watchdog. Nat. Cell Biol. 2, E31–E36.
Burke, J.D., Platanias, L.C., Fish, E.N., 2014. Beta interferon regulation of glucose metabolism is PI3K/Akt dependent and important for antiviral activity against coxsackievirus B3. J. Virol. 88, 3485–3495.
Burnett, J.C., Rossi, J.J., Tiemann, K., 2011. Current progress of siRNA/shRNA therapeutics in clinical trials. Biotech. J. 6, 1130–1146.
Carty, M., Reinert, L., Paludan, S.R., Bowie, A.G., 2014. Innate antiviral signalling in the central nervous system. Trends Immunol. 35, 79–87.
Chi, X.J., et al., 2013. Interaction domain between glycoproteins gB and gH of Marek's disease virus and identification of antiviral peptide with dual functions.

PloS One 8, e0054761.
Chiang, C., et al., 2015. Sequence-specific modifications enhance the broad-spectrum antiviral response activated by RIG-I agonists. J. Virol. 89, 8011–8025.
Cui, J., et al., 2010. NLRC5 negatively regulates the NF-kappaB and type I interferon signaling pathways. Cell 141, 483–496.
Cui, J., et al., 2014. USP3 inhibits type I interferon signaling by deubiquitinating RIG-I-like receptors. Cell Res. 24, 400–416.
Das, R.M., et al., 2006. A robust system for RNA interference in the chicken using a modified microRNA operon. Dev. Biol. 294, 554–563.
DeVincenzo, J.P., 2012. The promise, pitfalls and progress of RNA-interference-based antiviral therapy for respiratory viruses. Antivir. Ther. 17, 213–225.
Everett, R.D., Young, D.F., Randall, R.E., Orr, A., 2008. STAT-1- and IRF-3-dependent pathways are not essential for repression of ICP0-null mutant herpes simplex virus type 1 in human fibroblasts. J. Virol. 82, 8871–8881.
Fan, Y., et al., 2014. USP21 negatively regulates antiviral response by acting as a RIG-I deubiquitinase. J. Exper. Med. 211, 313–328.
Gack, M.U., et al., 2007. TRIM25 RING-finger E3 ubiquitin ligase is essential for RIG-I-mediated antiviral activity. Nature 446, 916–920.
Ge, Q., McManus, M.T., Nguyen, T., Shen, C.H., Sharp, P.A., Eisen, H.N., Chen, J., 2003. RNA interference of influenza virus production by directly targeting mRNA for degradation and indirectly inhibiting all viral RNA transcription. Proc. Natl. Acad. Sci. U. S. A. 100, 2718–2723.
Goulet, M.L., et al., 2013. Systems analysis of a RIG-I agonist inducing broad spectrum inhibition of virus infectivity. PLoS Pathog. 9, e1003298.
Hilton, L., et al., 2006. The NPro product of bovine viral diarrhea virus inhibits DNA binding by interferon regulatory factor 3 and targets it for proteasomal degradation. J. Virol. 80, 11723–11732.
Huang, D.D., 2008. The potential of RNA interference-based therapies for viral infections. Curr. HIV-AIDS Rep. 5, 33–39.
Jain, B., Jain, A., 2015. Taming influenza virus: role of antisense technology. Curr. Mol. Med. 15, 433–445.
Kalt, I., Levy, A., Borodianskiy-Shteinberg, T., Sarid, R., 2012. Nucleolar localization of GLTSCR2/PICT-1 is mediated by multiple unique nucleolar localization sequences. PloS One 7, e30825.
Lan, N.T., Yamaguchi, R., Kai, K., Uchida, K., Kato, A., Tateyama, S., 2005. The growth profiles of three types of canine distemper virus on Vero cells expressing canine signaling lymphocyte activation molecule. J. Vet. Med. Sci. 67, 491–495.
Li, C.G., Tang, W., Chi, X.J., Dong, Z.M., Wang, X.X., Wang, X.J., 2013. Cholesterol tag at N-terminal of the relatively broad spectrum of fusion inhibitory-peptide targets earlier stage of fusion glycoprotein activation and increases peptide's antiviral potency in vivo. J. Virol. 87, 9223–9232.
Lin, W., et al., 2016. Syndecan-4 negatively regulates antiviral signalling by mediating RIG-I deubiquitination via CYLD. Nat. Commun. 7, 11848.
Ling, Z., Tran, K.C., Teng, M.N., 2009. Human respiratory syncytial virus nonstructural protein NS2 antagonizes the activation of beta interferon transcription by interacting with RIG-I. J. Virol. 83, 3734–3742.
Liu, Y., et al., 2016. RIG-I mediated STING up-regulation restricts HSV-1 infection. J. Virol. 90, 9406–9419.
Masatani, T., et al., 2010. Rabies virus nucleoprotein functions to evade activation of the RIG-I-mediated antiviral response. J. Virol. 84, 4002–4012.
McSharry, B.P., Forbes, S.K., Avdic, S., Randall, R.E., Wilkinson, G.W., Abendroth, A., Slobedman, B., 2015. Abrogation of the interferon response promotes more efficient human cytomegalovirus replication. J. Virol. 89, 1479–1483.
Ng, D., Gommerman, J.L., 2013. The regulation of immune responses by DC derived type I IFN. Front. Immunol. 4, 94.
Okahara, F., Ikawa, H., Kanaho, Y., Maehama, T., 2004. Regulation of PTEN phosphorylation and stability by a tumor suppressor candidate protein. J. Bol. Chem. 279, 45300–45303.
Reissmann, S., 2014. Cell penetration: scope and limitations by the application of cell-penetrating peptides. J. Pep. Sci. 20, 760–784.
Reyes-Turcu, F.E., Ventii, K.H., Wilkinson, K.D., 2009. Regulation and cellular roles of ubiquitin-specific deubiquitinating enzymes. Annu. Rev. Biochem. 78, 363–397.
Rizzuti, M., Nizzardo, M., Zanetta, C., Ramirez, A., Corti, S., 2015. Therapeutic applications of the cell-penetrating HIV-1 Tat peptide. Drug Discov. Today 20, 76–85.
Sasaki, M., et al., 2011. Regulation of the MDM2-P53 pathway and tumor growth by PICT1 via nucleolar RPL11. Nat. Med. 17, 944–951.
Schneider, W.M., Chevillotte, M.D., Rice, C.M., 2014. Interferon-stimulated genes: a complex web of host defenses. Annu. Rev. Immunol. 32, 513–545.
Spurgers, K.B., Sharkey, C.M., Warfield, K.L., Bavari, S., 2008. Oligonucleotide antiviral therapeutics: antisense and RNA interference for highly pathogenic RNA viruses. Antivir. Res. 78, 26–36.
Sun, D., et al., 2015. Analysis of protein expression changes of the Vero E6 cells infected with classic PEDV strain CV777 by using quantitative proteomic technique. J. Virol. Methods 218, 27–39.
Sui, G., et al., 2002. A DNA vector-based RNAi technology to suppress gene expression in mammalian cells. Proc. Natl. Acad. Sci. U. S. A. 99, 5515–5520.
Tawaratsumida, K., Phan, V., Hrincius, E.R., High, A.A., Webby, R., Redecke, V., Hacker, H., 2014. Quantitative proteomic analysis of the influenza A virus nonstructural proteins NS1 and NS2 during natural cell infection identifies PACT as an NS1 target protein and antiviral host factor. J. Virol. 88, 9038–9048.
Wang, X., Patenode, C., Roizman, B., 2011. US3 protein kinase of HSV-1 cycles between the cytoplasm and nucleus and interacts with programmed cell death protein 4 (PDCD4) to block apoptosis. Proc. Natl. Acad. Sci. U. S. A. 108, 14632–14636.
Wang, B., Zhang, H., Zhu, M., Luo, Z., Peng, Y., 2012. MEK1-ERKs signal cascade is required for the replication of enterovirus 71 (EV71). Antiv. Res. 93, 110–117.
Wang, J., et al., 2015. Development of a reverse genetics system based on RNA polymerase II for Newcastle disease virus genotype VII. Virus Genes 50, 152–155.
Wang, P., et al., 2016a. The nucleolar protein GLTSCR2 is required for efficient viral replication. Sci. Rep. 6, 36226.
Wang, G., et al., 2016b. Non-thermal plasma for inactivated-vaccine preparation. Vaccine 34, 1126–1132.
Wilkins, C., Gale Jr., M., 2010. Recognition of viruses by cytoplasmic sensors. Curr. Opin. Immunol. 22, 41–47.
Xing, J., Wang, S., Lin, R., Mossman, K.L., Zheng, C., 2012. Herpes simplex virus 1 tegument protein US11 downmodulates the RLR signaling pathway via direct interaction with RIG-I and MDA-5. J. Virol. 86, 3528–3540.
Xing, Y., et al., 2013. The papain-like protease of porcine epidemic diarrhea virus negatively regulates type I interferon pathway by acting as a viral deubiquitinase. J. Gen. Virol. 94, 1554–1567.
Xu, G., Yang, F., Ding, C.L., Wang, J., Zhao, P., Wang, W., Ren, H., 2014. MiR-221 accentuates IFN's anti-HCV effect by downregulating SOCS1 and SOCS3. Virology 462–463, 343–350.
Yan, J., Li, Q., Mao, A.P., Hu, M.M., Shu, H.B., 2014. TRIM4 modulates type I interferon induction and cellular antiviral response by targeting RIG-I for K63-linked ubiquitination. J. Mol. Cell Biol. 6, 154–163.
Yi, M., Lemon, S.M., 2004. Adaptive mutations producing efficient replication of genotype 1a hepatitis C virus RNA in normal Huh7 cells. J. Virol. 78, 7904–7915.
Yim, J.H., et al., 2007. The putative tumor suppressor gene GLTSCR2 induces PTEN-modulated cell death. Cell Death. Differ. 14, 1872–1879.
Yin, R., et al., 2010. Inhibition of Newcastle disease virus replication by RNA interference targeting the matrix protein gene in chicken embryo fibroblasts. J. Virol. Methods 167, 107–111.
Young, D.F., et al., 2003. Virus replication in engineered human cells that do not respond to interferons. J. Virol. 77, 2174–2181.
Yuan, X., et al., 2012. Genetic and biological characterizations of a Newcastle disease virus from swine in China. Virol. J. 9, 129.
Yue, H., et al., 2009. Short hairpin RNA targeting NP mRNA inhibiting Newcastle disease virus production and other viral structural mRNA transcription. Virus Genes 38, 143–148.
Zhang, H., et al., 2015. Ubiquitin-specific protease 15 negatively regulates virus-induced type I interferon signaling via catalytically-dependent and -independent mechanisms. Sci. Rep. 5, 11220.